

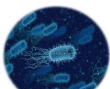
Bistability in the Dynamics of Bacterial Restriction-Modification Systems

Magdalena Djordjevic ¹ Lidija Zivkovic ¹ Hong Yu-OU ²
Marko Djordjevic ³

¹Institute of Physics Belgrade

²Shanghai Yiao Tong

³UB-Faculty of Biology



Outline

- 1 Bistability introduction
- 2 Mathematical model
 - System regulation
 - Dynamical equations
- 3 Biology and experiment comparison
 - Significance of R-M systems
 - Comparison with Esp1396l data and predictions for AhdI
 - EcoRV predictions
 - Cusp catastrophe surface
 - Stochastic simulations
- 4 Conclusion and discussion
 - Theory
 - Biology
 - Graphical summary

Stable and Unstable Steady States

- Stable: a perturbation returns the system to equilibrium
- Unstable: a small perturbation drives the system away from equilibrium

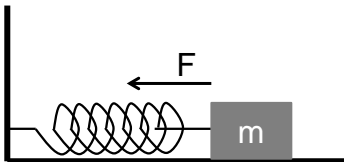


Figure: Stable steady state

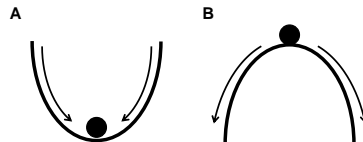
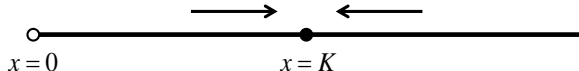


Figure: A: Stable steady state, B: Unstable steady state

Logistic Growth Model

- $\frac{dN}{dt} = rN(1 - \frac{N}{K})$
- We plot N on the horizontal axis and indicate the sign of dN/dt
- An open circle denotes an unstable, and a filled circle a stable, steady state

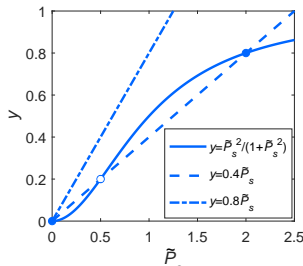


Cooperative Positive Feedback

$$\phi(P) = \phi_m \frac{(P/K)^2}{1 + (P/K)^2}, \quad (1)$$

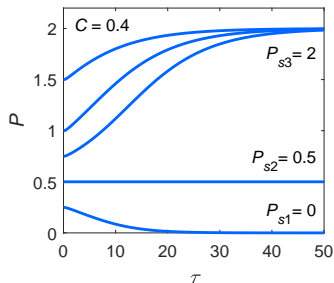
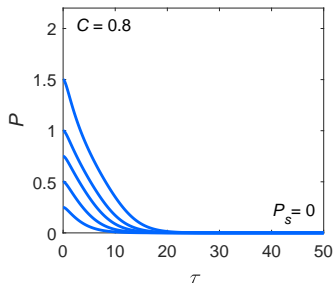
$$\frac{dP}{dt} = \phi(P) - \beta P \quad (2)$$

- Cooperative autoregulation leads to bistability:



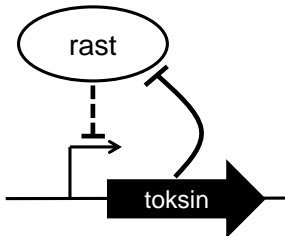
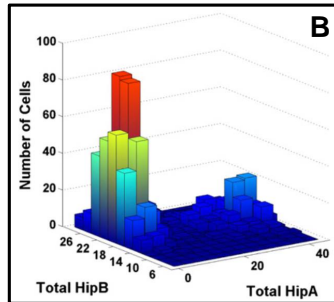
Dynamics of Monostable and Bistable Systems

- A monostable system ends in the same single steady state regardless of initial conditions.
- In a bistable system, depending on initial conditions, the system can end in one of two steady states.



Bistability in Antibiotic Persistence

- Effective positive feedback
- In an isogenic population, two subpopulations emerge: one with low toxin levels (normal growth) and one with high toxin levels (persister cells)

A**B**

C regulation

- Start from one transcription factor (control protein "C")
- C dimerizes and binds to its promoter as a dimmer
- Binding leads to both positive and negative feedback (next slide)

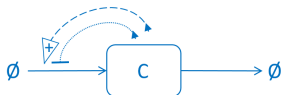


Figure: C autoregulation

General dynamics:

Total C generated by transcription ϕ diluted by cell division (λ):

$$\frac{dC_t}{dt} = n\phi(C) - \lambda C_t$$

Dimmer formation (with $K_{d,1}$)

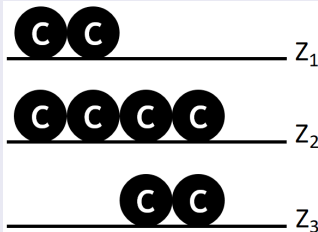
$$D = C^2 / K_{d,1}$$

$$C_t = C + 2D$$

$$C = \frac{K_{d,1}}{4} \left(\sqrt{1 + \frac{8C_t}{K_{d,1}}} - 1 \right)$$

Dimerization and transcription in quasi-equilibrium. n - copy number

Promoter configurations:



Transcription activity:

$$\phi(C) = \phi_l + \phi_m \frac{Z_1}{1 + Z_1 + Z_2 + Z_3}$$

$$\phi(C) = \phi_l + \phi_m \frac{C^2/(K_{d,1}K_{d,2})}{1 + C^2/(K_{d,1}K_{d,2}) + (\omega C^4)/(pK_{d,1}^2 K_{d,2}^2) + C^2/(pK_{d,1}K_{d,2})}$$

$K_{d,2}$	$K_{d,3}$	$K_{d,23}$
left	right	left and right

Table: C binding

weight	expression	effect
Z_1	$C^2/(K_{d,1}K_{d,2})$	activate
Z_2	$(\omega C^4)/(pK_{d,1}^2 K_{d,2}^2)$	repress
Z_3	$C^2/(pK_{d,1}K_{d,2})$	repress

Table: Statistical weights

Rescaled dynamics:

$$\frac{d\tilde{C}_t}{d\tau} = s + \frac{\tilde{C}^2}{1 + \tilde{C}^2(1 + 1/p) + \omega/p\tilde{C}^2} - \tilde{C}_t/r, \text{ with } \tilde{C} = \alpha/4(\sqrt{1 + 8\tilde{C}_t/\alpha} - 1)$$

Dynamics description

Complex system dynamics can be condensed to five parameters with clear biophysical interpretation directly related to experimentally measurable quantities. *alpha*, *p*, and *omega* are fixed for a given R-M system, but change between different systems. *r* and *s* depend both on the system and external conditions (e.g., cell growth rate controlling lambda).

parameter	expression	interpretation
α	$\sqrt{K_{d,1}/K_{d,2}}$	dimmer formation
p	$K_{d,3}/K_{d,2}$	proximal to distal binding strength
ω	$K_{d,2}K_{d,3}/K_{d,23}$	binding cooperativity
r	$(n\phi_m)/(\lambda\sqrt{K_{d,1}K_{d,2}})$	overall C expression strength
s	ϕ_l/ϕ_m	promoter leakage

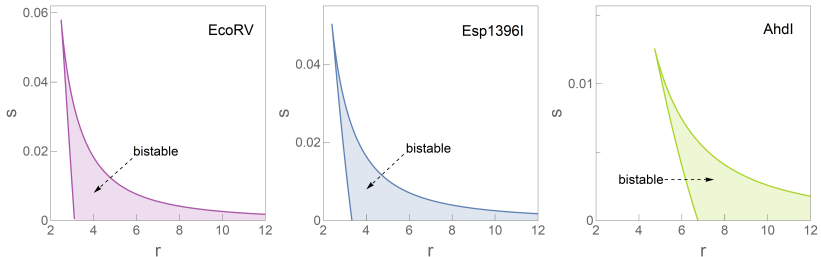
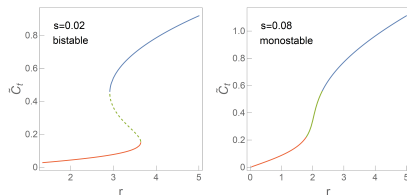
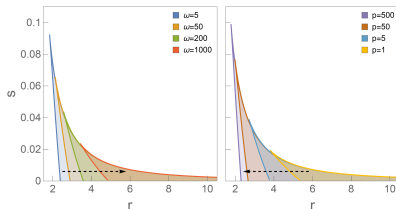


Figure: Stability diagrams for different R-M systems

Analytical derivation of the stability diagram (here highly nontrivial!)

State of the art is to put the bifurcation parameters on a grid (here r and s) so that for every grid point, stability has to be calculated - and then repeated for every combination of the system parameters (here α , ω and p). With the analytical derivation, one just has to re-plot the curves!

Dynamical equations

Figure: r bifurcation diagrams

Change of the bistability region:

Bistability is promoted by:

- small ω (cooperativity)
- large p (stronger activation binding)

Intuition: Positive feedback promotes, and negative abolishes bistability!

Changing r and s

- Small promoter leakage (s) promotes bistability
- Bistability at intermediate r values

Significance of R-M systems

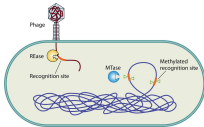


Figure: R-M as a rudimentary Bacterial Defense System



Figure: R-M as a rudimentary Bacterial Defense System. From PMID:23471617

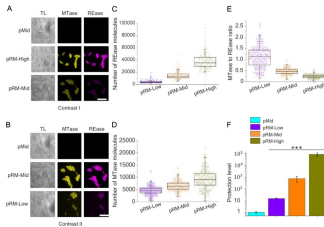


Figure: from PMID:36477001

R-M modulates HGT barrier

M/R changes significantly with system parameters. The plasmid copy number (proportional to our *r*) is changed in the experiment. With this barrier to HGT (protection against bacteriophages) is modulated.

Comparison with Esp1396I data and predictions for AhdI

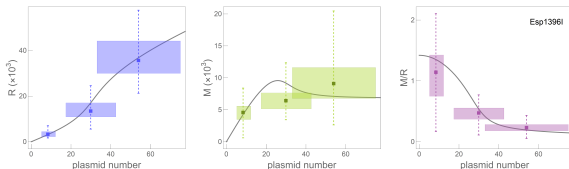


Figure: Esp1396I: Model fit to experimental data (two free parameters.)

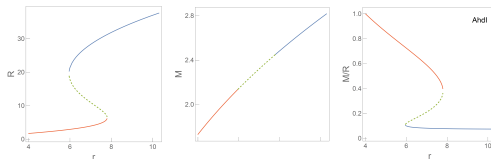


Figure: AhdI: Prediction based on s inferred from the experiment

Esp 1396I monostable, AhdI predicted bistable!



EcoRV predictions

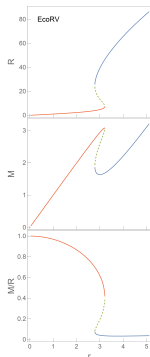


Figure: EcoRV bistable prediction

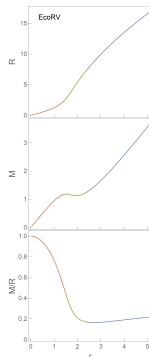


Figure: EcoRV monostable predictions

EcoRV predictions

EcoRV s value is not known from the experiment. However, despite quite different regulations (divergent promoters), R/M dependence is predicted to be similar to Ahdl and EcoRV.

Cusp catastrophe surface

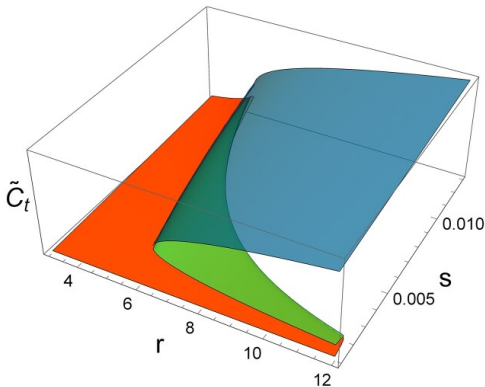


Figure: Cusp catastrophe surface

Cusp catastrophe surface

The three axes correspond to r , S (forming a horizontal plane) and \tilde{C}_t on the vertical axis. The upper (blue) surface corresponds to the high R state, and the lower (red) surface corresponds to the low R state. The middle (green) surface that connects the lower (red) and the upper (blue) surface corresponds to the unstable steady state. The green surface is inaccessible due to hysteresis behavior.

Stochastic simulations

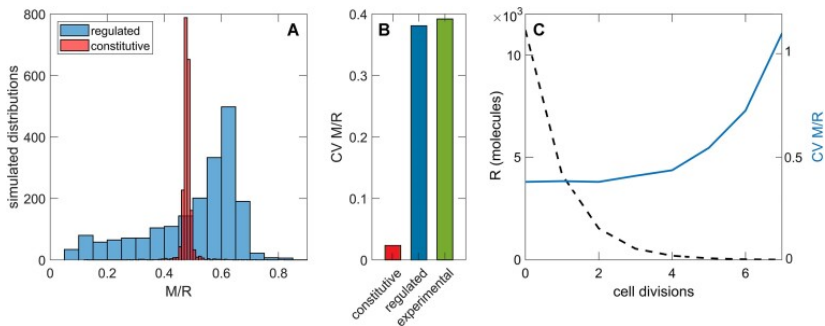


Figure: Stochastic simulation

For monostable systems stochastic effects enhance heterogeneity and modulate post-segregational killing

Conclusions theory

Developed analytical model directly applicable to diverse C-controlled R-M systems

- Change three experimentally directly measurable parameters (α , ω and ρ) that are fixed for a given system.
- Re-plot equations with these three parameters to obtain a stability diagram.
- Place your system in the stability diagram based on just another two systems (and condition) dependent parameters (r and s).
- From this, perform straightforward numerical calculations to obtain experimentally measurable quantities.
- Behavior of a complex class of systems is condensed to just five parameters and a straightforward numerical procedure.

Conclusions biology

Explain experimental data and predict different qualitative dynamics of the system

- Model agrees well with measured Esp1396I data, with the absence of bistability (at least under experimental conditions).
- For AhdI bistable regime is predicted.
- EcoRV shows similar qualitative behavior as Esp1396I and AhdI.
- Consequences of bistability in R-M systems remain to be understood!
- In analogy to possible roles of TA systems in antibiotic persistence, could R-M system regulation lead to a subpopulation that can more easily acquire foreign genes (including virulence, antibiotic resistance, etc. variants)?

Graphical summary

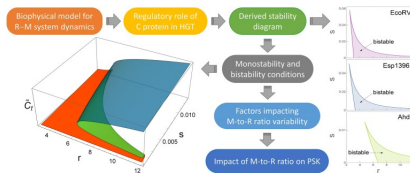


Figure: Graphical summary

Overall

Overall, heterogeneity in the expression of mechanistically similar R-M systems—despite their markedly different biophysical parameters—can arise either through bistability or enhanced noise.

Reference

Djordjevic, M., Zivkovic, L., Ou, H. Y., Djordjevic, M. (2025). Nonlinear regulatory dynamics of bacterial restriction-modification systems modulates horizontal gene transfer susceptibility. *Nucleic Acids Research*, 53(2), gkae1322.

kacAT configuration and experimental observations

kacAT properties

- *kacAT* architecture generally similar to other Type II systems
- Large binding cooperativity where complex is formed by 2T and 4A
- Strong system response to stress
- However, no induction of spontaneous persistence!
- Antitoxin is degraded in response to stress

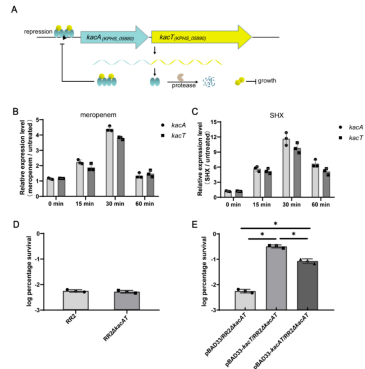


Figure: kacAT regulation and experimental results [1]

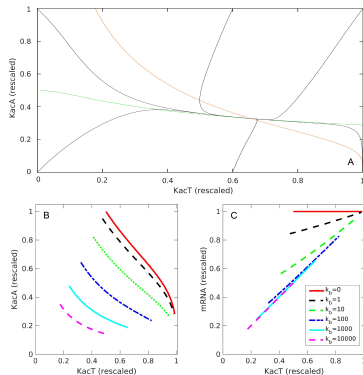
Mathematical model of the system dynamics [1]:

$$\frac{dA}{d\tau} = \frac{2k\phi}{1 + K_b A^4 B^2} - (1 + \delta\lambda)A - 4A^4 B^2$$

$$\frac{dB}{d\tau} = \frac{k\phi}{1 + K_b A^4 B^2} - B - 2A^4 B^2$$

Model explains:

- Reduction of the [KacA]:[KacT] ratio upon antibiotic application.
- Large increase in *kacAT* transcripts induced by antibiotics.
- KacAT overexpression induces antibiotic stress tolerance, whereas *kacAT* deletion does not affect this tolerance.





Persister emergence model assumption

- Why *kacAT* deletion does not lead to spontaneous persister formation despite previous theoretical predictions?
- Theoretical studies assume cooperative (joint) action of several TAs.

Only one system in the same family as *kacAT* strongly preferred!

Also, statistically significant negative correlations between different clades for which experiments indicate their cross-talk [2]

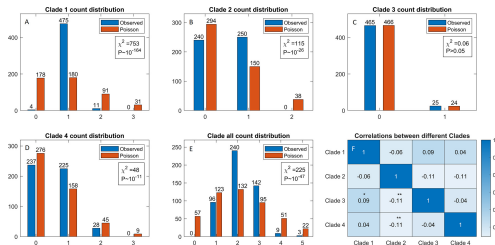


Figure: Statistical analysis of GNAT-RHH TA pairs in *K. pneumoniae* strains.

References

- [1] Peifei Li, Ying-Xian Goh, Bojana Ilic, Cui Tai, Zixin Deng, Zhaoyan Chen, Marko Djordjevic, and Hong-Yu Ou. Antibiotic-induced degradation of antitoxin enhances the transcription of acetyltransferase-type toxin-antitoxin operon. *The Journal of Antimicrobial Chemotherapy*, 78(4).
- [2] Ying-Xian Goh, Peifei Li, Meng Wang, Marko Djordjevic, Cui Tai, Hui Wang, Zixin Deng, Zhaoyan Chen, and Hong-Yu Ou. Comparative Analysis of Diverse Acetyltransferase-Type Toxin-Antitoxin Loci in *Klebsiella pneumoniae*. *Microbiology Spectrum*, 10(4).

Acknowledgments

This work is collaboration with Peifei Li, Ying-Xian Goh, Cui Tai, Zixin Deng, Zhaoyan Chen, Meng Wang and Hui Wang. Work was also supported by Science and Technology Commission of Shanghai Municipality (Grant 19430750600), the National Natural Science Foundation of China (Grant 32070572), the Medical Excellence Award Funded from the First Affiliated Hospital of Guangxi Medical University (XK2019025).